

Exact and asymptotic solutions of the mixed quantum-classical Liouville equation

Chun-Cheng Wan and Jeremy Schofield^{a)}

Chemical Physics Theory Group, Department of Chemistry, University of Toronto, Toronto, Ontario, M5S 3H6, Canada

(Received 30 September 1999; accepted 9 December 1999)

In this article, an exact surface-hopping procedure and an approximate asymptotic method for performing molecular dynamics based on a mixed quantum-classical Liouville equation [J. Chem. Phys. **110**, 8919 (1999)] for partially Wigner transformed dynamical variables of a coupled quantum subsystem and classical bath are elaborated. The methods are based upon writing the equations of motion in a basis set in which quantum transitions do not alter the classical trajectory, and therefore avoid *ad-hoc* momentum jump approximations and are free of singular kernels associated with sampling momenta.² Results obtained utilizing the new trajectory methods are presented for a model two-level system bilinearly coupled to a classical harmonic oscillator. These results are compared to results obtained from standard methods of performing mixed quantum-classical dynamics. The new methods perform well for the model system over a wide range of initial kinetic energies. © 2000 American Institute of Physics. [S0021-9606(00)01109-0]

I. INTRODUCTION

A number of procedures have been proposed recently^{1–10} for performing molecular dynamics simulations of condensed phase and molecular systems in which the Born–Oppenheimer approximation breaks down. In such systems, the incorporation of quantum effects into the description of the dynamical evolution of the system is necessary. Quantum effects are particularly important in many chemical systems containing hydrogen atoms where the nuclear motion evolves on multiple energy surfaces which are coupled.

One approach to the problem of incorporating quantum effects in molecular dynamics is based upon semi-classical methods,¹¹ such as the initial-value representation (IVR)¹² and its simplified versions (LSC-IVR).¹³ Although the semi-classical methods are appealing because they treat the classical and quantum degrees of freedom on equal footing, accurate calculations using IVR methods tend to be computationally intensive due to the slow convergence of oscillatory integrands. Furthermore, the approximations made to obtain tractable expressions for transition probabilities and time-correlation functions are fairly subtle and difficult to control.

Another common approach of performing molecular dynamics simulations on mixed quantum-classical systems is to concoct accurate methods of combining classical methods for the “classical” system while retaining a minimal level of quantum description for the remainder of the system. These methods are usually based on either *ad-hoc* rules for the mixed quantum-classical system evolution,^{3,4} or on stationary-phase approximations of reduced path integral propagators.^{14,5–7} The latter methods are typically plagued by problems of norm conservation. Mixed quantum-classical methods are often implemented through a stochastic

“surface-hopping” algorithm¹⁵ in which the classical evolution occurs with Hellmann–Feynman forces on a single, statistically chosen adiabatic energy surface.

In a recent article, Kapral and Ciccotti¹ derived equations of motion for a mixed quantum-classical system based on a systematic expansion in the ratio of the masses of the quantum and classical degrees of freedom of the exact evolution equations. By retaining terms up to linear order in $\epsilon = (m/M)^{1/2}$, where m and M are the masses of the quantum and classical degrees of freedom respectively, they obtained a quantum-classical Liouville equation that accounts for the coupled evolution of the quantum subsystem and the classical “bath.” In this article, we examine exact and approximate surface-hopping algorithms for carrying out molecular dynamics simulations based on the quantum-classical Liouville equation. The methods presented here utilize a representation for the quantum subsystem in which quantum transitions arise through a commutator-like super-operator which couples the quantum states while the classical degrees of freedom evolve. In this representation, which is outlined in Sec. II, all classical trajectories are smooth and free of momentum readjustments when the quantum subsystem changes state. In Sec. III, a stochastic surface-hopping algorithm for solving the coupled matrix equations in the “force basis” representation is presented. In Sec. IV, this algorithm is applied to a simple model system consisting of a two-level system bilinearly coupled to a massive harmonic oscillator, and the results obtained utilizing the new stochastic algorithm are compared to the exact solution obtained via fast Fourier transform methods. Issues of convergence of the algorithm and possible extensions of the method are also discussed in this section. In Sec. V, an asymptotically exact deterministic method of solving the mixed quantum-classical Liouville equation is presented. This new method is particularly useful for systems of small kinetic energy where clas-

^{a)}Electronic mail: jmschofi@chem.utoronto.ca

sically forbidden transitions play an important role in the dynamics. Furthermore, the method offers a systematic approach to investigate issues of numerical accuracy. Calculations performed with the method are compared to results obtained by stochastic methods for the model system. The conclusions of the study of the method are given in Sec. VI.

II. GENERAL FORMULATION

A. The quantum-classical Liouville equation

Consider a general quantum system consisting of n quantum particles of mass m and N particles of mass M with a Hamiltonian of the form

$$\hat{H} = \frac{\hat{P}^2}{2M} + \frac{\hat{p}^2}{2m} + \hat{V}(\hat{q}, \hat{Q}), \quad (1)$$

where \hat{P} , \hat{p} , \hat{Q} , and \hat{q} are vectors of momentum and position operators of the classical and quantum degrees of freedom. The total potential energy \hat{V} may be written as $\hat{V}_q(\hat{q}) + \hat{V}_{cl}(\hat{Q}) + \hat{V}_c(\hat{Q}, \hat{q})$, where the subscripts refer to the quantum, classical, and coupling terms in the potential energy. The evolution of any dynamical observable \hat{B} is given by the Heisenberg equation,

$$\frac{d\hat{B}}{dt} = \frac{i}{\hbar} [\hat{H}, \hat{B}]. \quad (2)$$

In order to focus on the limit in which the particles with mass M , with $M \gg m$, are treated classically, it is convenient to perform a partial Wigner transform with respect to the classical degree of freedom \hat{Q} defined as

$$\hat{B}_w(R, P) = \frac{1}{(2\pi\hbar)^{3N/2}} \int dz e^{iP \cdot z/\hbar} \left\langle R - \frac{z}{2} \left| \hat{B} \right| R + \frac{z}{2} \right\rangle, \quad (3)$$

where R is the coordinate representation of the operator \hat{Q} . Note that $\hat{B}_w(R, P)$ is still an operator in the quantum subspace. In the limit in which the masses of the bath (classical) particles are much larger than the quantum particle masses, a small parameter $\epsilon = (m/M)^{1/2}$ may be defined and used to perturbatively order terms¹ in the equations of motion for a partially Wigner transformed dynamical observable $\hat{B}_w(R, P)$. If terms up to first order in ϵ are retained in the full equation of motion, a Liouville equation for the mixed quantum-classical system is obtained:¹

$$\begin{aligned} \frac{d\hat{B}_w(R, P, t)}{dt} &= \frac{i}{\hbar} [\hat{H}_w(R, P), \hat{B}_w(R, P, t)] \\ &\quad - \frac{1}{2} (\{\hat{H}_w(R, P), \hat{B}_w(R, P, t)\} \\ &\quad - \{\hat{B}_w(R, P, t), \hat{H}_w(R, P)\}) \\ &= i\mathcal{L}\hat{B}_w(R, P, t), \end{aligned} \quad (4)$$

where the Poisson bracket notation in Eq. (4) signifies

$$\begin{aligned} \{\hat{H}_w(R, P), \hat{B}_w(R, P)\} &= \frac{\partial \hat{H}_w(R, P)}{\partial R} \cdot \frac{\partial \hat{B}_w(R, P)}{\partial P} \\ &\quad - \frac{\partial \hat{H}_w(R, P)}{\partial P} \cdot \frac{\partial \hat{B}_w(R, P)}{\partial R}, \end{aligned} \quad (5)$$

and the partial Wigner transform of the Hamiltonian is

$$\hat{H}_w(R, P) = \frac{P^2}{2M} + \frac{\hat{p}^2}{2m} + \hat{V}_w(R, \hat{q}) = \frac{P^2}{2M} + \hat{h}_w(R, P). \quad (6)$$

It is important to note that in (4), total energy is conserved by construction regardless of the choice of quantum subsystem representation. Similarly, the evolution equation for the partial Wigner transform $\hat{\rho}_w$ of the full density matrix $\hat{\rho}$ can be written as

$$\frac{\partial \hat{\rho}_w(R, P, t)}{\partial t} = -i\mathcal{L}\hat{\rho}_w(R, P, t). \quad (7)$$

Correlation functions can also be expanded to linear order in the small parameter ϵ for the mixed quantum-classical system. Consider the symmetrized correlation function,

$$\langle \hat{A}(t)\hat{B} \rangle^s = \frac{1}{2} \text{Tr}\{\hat{A}(t)\hat{B} + \hat{B}\hat{A}(t)\} \quad (8)$$

$$= \frac{1}{2} \sum_{\alpha} \int dR dP ((\hat{A}(t)\hat{B}\hat{\rho})_w + (\hat{\rho}\hat{B}\hat{A}(t))_w)^{\alpha\alpha}, \quad (9)$$

where the Tr operator is the trace over the quantum system states, α are some complete set of quantum sub-system states, and $(\hat{A}\hat{B})_w$ is the partial Wigner transform of the product operator $\hat{A}\hat{B}$. Using the relation that to order ϵ^2 ,

$$(\hat{A}\hat{B})_w = \hat{A}_w(R, P)\hat{B}_w(R, P) + \frac{\hbar}{2i} \{\hat{A}_w(R, P), \hat{B}_w(R, P)\}, \quad (10)$$

in Eq. (9), we obtain

$$\begin{aligned} \langle \hat{A}(t)\hat{B} \rangle^s &= \frac{1}{2} \sum_{\alpha} \int dR dP (\hat{A}_w(t)\hat{B}_w\hat{\rho}_w + \hat{\rho}_w\hat{B}_w\hat{A}_w(t))^{\alpha\alpha} \\ &\quad + \frac{\hbar}{4i} \sum_{\alpha} \int dR dP (\hat{A}_w(t)\{\hat{B}_w, \hat{\rho}_w\} \\ &\quad + \{\hat{\rho}_w, \hat{B}_w\}\hat{A}_w(t))^{\alpha\alpha}. \end{aligned} \quad (12)$$

If \hat{B} is a purely quantum operator so that $\hat{B}_w = \hat{B}$, then only the first term of (12) survives. Similarly, the term proportional to \hbar also vanishes if \hat{B} is a purely classical operator due to a cancellation in the Poisson bracket terms. It also vanishes if \hat{B} is the unity operator (i.e., the average $\langle \hat{A}(t) \rangle$). Once again, it is readily apparent that both the average energy and total populations in the set of quantum states α is conserved exactly. This is in contrast to methods based upon stationary phase approximations of path integral expressions of the reduced propagator⁷ in which the approximate propagator is no longer unitary, leading to a full system dynamics which does not conserve the norm.

Henceforth, as in Eq. (12), we shall drop to R and P dependence of partially Wigner transformed operators for notational simplicity unless the explicit dependence is necessary for clarity.

B. Basis set representations

Equation (4) is solved by representing the quantum operators of the subsystem in a complete basis set. One common, and convenient, choice of basis set is the set of ‘‘adiabatic’’ states $|\tilde{\alpha}(R)\rangle$ which diagonalize the operator \hat{h}_w defined in Eq. (6):

$$\hat{h}_w(R)|\tilde{\alpha}(R)\rangle = E_{\tilde{\alpha}}(R)|\tilde{\alpha}(R)\rangle. \quad (13)$$

Note that due to the parametric dependence of the operator \hat{h}_w on R , the basis set is R dependent. Taking matrix elements of Eq. (4), one obtains¹ the equation of motion for the matrix element $B_w^{\tilde{\alpha}\tilde{\beta}}(t)$,

$$\frac{dB_w^{\tilde{\alpha}\tilde{\beta}}(t)}{dt} = i\mathcal{L}_{\tilde{\alpha}\tilde{\beta},\tilde{\alpha}'\tilde{\beta}'} B_w^{\tilde{\alpha}'\tilde{\beta}'}(t), \quad (14)$$

where the Liouville superoperator $i\mathcal{L}_{\tilde{\alpha}\tilde{\beta},\tilde{\alpha}'\tilde{\beta}'}$ is given by

$$\begin{aligned} i\mathcal{L}_{\tilde{\alpha}\tilde{\beta},\tilde{\alpha}'\tilde{\beta}'} &= i\omega_{\tilde{\alpha}\tilde{\beta}}\delta_{\tilde{\alpha}\tilde{\alpha}'}\delta_{\tilde{\beta}\tilde{\beta}'} + \frac{P}{M} \cdot \frac{\partial}{\partial R} \delta_{\tilde{\alpha}\tilde{\alpha}'}\delta_{\tilde{\beta}\tilde{\beta}'} \\ &+ \frac{P}{M} \cdot (\mathbf{d}_{\tilde{\alpha}\tilde{\alpha}'}\delta_{\tilde{\beta}\tilde{\beta}'} - \mathbf{d}_{\tilde{\beta}\tilde{\beta}'}\delta_{\tilde{\alpha}\tilde{\alpha}'}) \\ &+ \frac{1}{2}(\mathbf{F}_w^{\tilde{\alpha}\tilde{\alpha}'}\delta_{\tilde{\beta}\tilde{\beta}'} + \mathbf{F}_w^{\tilde{\beta}'\tilde{\beta}}\delta_{\tilde{\alpha}\tilde{\alpha}'}) \cdot \frac{\partial}{\partial P}, \end{aligned} \quad (15)$$

with $\omega(R) = (E_{\tilde{\alpha}}(R) - E_{\tilde{\beta}})/\hbar$. In Eq. (15), quantum state couplings arise through the off-diagonal matrix terms of the nonadiabatic coupling matrix $\mathbf{d}_{\tilde{\alpha}\tilde{\alpha}'}$ given by

$$\mathbf{d}_{\tilde{\alpha}\tilde{\alpha}'} = \langle \tilde{\alpha}(R) | \frac{\partial}{\partial R} | \tilde{\alpha}'(R) \rangle, \quad (16)$$

and the off-diagonal ‘‘force,’’

$$\mathbf{F}_w^{\tilde{\alpha}\tilde{\alpha}'} = -\langle \tilde{\alpha}(R) | \frac{\partial \hat{H}_w}{\partial R} | \tilde{\alpha}'(R) \rangle. \quad (17)$$

The diagonal elements of the force matrix are the Hellmann–Feynman forces,

$$\mathbf{F}_w^{\tilde{\alpha}\tilde{\alpha}} = -\frac{\partial E_{\tilde{\alpha}}(R)}{\partial R}, \quad (18)$$

and the off-diagonal elements can be expressed¹ in terms of the nonadiabatic coupling matrix \mathbf{d} . Equation (14) can be conveniently written using supermatrix notation in which all matrix elements $B_w^{\tilde{\alpha}\tilde{\beta}}$ are represented in a single supervector $B_w^{\tilde{\mu}}$, with $\tilde{\mu}$ representing the pair $(\tilde{\alpha}, \tilde{\beta})$ as

$$\frac{dB_w^{\tilde{\mu}}(t)}{dt} = i\mathcal{L}_{\tilde{\mu},\tilde{\nu}} B_w^{\tilde{\nu}}(t), \quad (19)$$

and formally solved to obtain

$$B_w^{\tilde{\mu}}(t) = (e^{i\mathcal{L}t})_{\tilde{\mu}\tilde{\nu}} B_w^{\tilde{\nu}}(0). \quad (20)$$

Equation (20) can be used as a starting point for exact solutions of the mixed quantum-classical equations of motion in the adiabatic basis. For systems which retain characteristics of the adiabatic ground state dynamics and involve only a small number of adiabatic energy surfaces and forces, the matrix equation can be truncated to include only a few states. For such weakly nonadiabatic systems, the matrix indices $\tilde{\mu}$ run over a small set of indices, resulting in a tractable system of equations.

Although Eq. (20) can be solved by brute force diagonalization techniques for systems with few classical degrees of freedom, larger systems require somewhat more sophisticated approaches. A number of methods of tackling the numerical solution of (20) are potentially feasible. One possibility is to separate the Liouville supermatrix operator $i\mathcal{L}$ into diagonal $i\mathcal{L}^{cl}$ and off-diagonal $i\mathcal{L}^Q$ components. Based on symmetries of the superoperator matrices, it can be shown that each component of the supermatrix operator has purely imaginary eigenvalues, so that the Trotter product formula,¹⁶

$$e^{-i(\mathcal{L}^{cl} + \mathcal{L}^Q)t} = (e^{-i\mathcal{L}^{cl}t/2N_t} e^{-i\mathcal{L}^Q t/N_t} e^{-i\mathcal{L}^{cl}t/2N_t})^{N_t} + O(N^{-2}), \quad (21)$$

may be applied to approximate propagation over the total time interval as propagation over N_t short time segments of duration Δt , with $t = N_t \Delta t$:

$$\begin{aligned} B_w(t) &= e^{i\mathcal{L}^{cl}\Delta t/2} M_{ad}(\Delta t) e^{i\mathcal{L}^{cl}\Delta t/2} \dots e^{i\mathcal{L}^{cl}\Delta t/2} \\ &\times M_{ad}(\Delta t) e^{i\mathcal{L}^{cl}\Delta t/2} B_w(0), \end{aligned} \quad (22)$$

with the off-diagonal matrix $M_{ad}(\Delta t)$ given by

$$M_{ad}^{\tilde{\mu}\tilde{\nu}}(\Delta t) = (e^{i\mathcal{L}^Q \Delta t})_{\tilde{\mu}\tilde{\nu}} \quad (23)$$

$$\approx \delta_{\tilde{\mu}\tilde{\nu}} + i\mathcal{L}_{\tilde{\mu}\tilde{\nu}}^Q \Delta t. \quad (24)$$

Using the form of the superoperator $i\mathcal{L}$ in Eq. (15), the off-diagonal part of the Liouville operator can be written as¹

$$\begin{aligned} i\mathcal{L}_{\tilde{\alpha}\tilde{\beta},\tilde{\alpha}'\tilde{\beta}'}^Q &= \frac{P}{M} \cdot \mathbf{d}_{\tilde{\alpha}\tilde{\alpha}'} \left(1 + \frac{1}{2} S_{\tilde{\alpha}\tilde{\alpha}'} \cdot \frac{\partial}{\partial P} \right) \delta_{\tilde{\beta}\tilde{\beta}'} + \frac{P}{M} \\ &\cdot \mathbf{d}_{\tilde{\beta}\tilde{\beta}'}^* \left(1 + \frac{1}{2} S_{\tilde{\beta}\tilde{\beta}'}^* \cdot \frac{\partial}{\partial P} \right) \delta_{\tilde{\alpha}\tilde{\alpha}'}, \end{aligned} \quad (25)$$

with ‘‘jump’’ matrix element

$$S_{\tilde{\alpha}\tilde{\alpha}'} = \frac{F_w^{\tilde{\alpha}\tilde{\alpha}'} - F_w^{\tilde{\alpha}\tilde{\alpha}} \delta_{\tilde{\alpha}\tilde{\alpha}'}}{P/M \cdot \mathbf{d}_{\tilde{\alpha}\tilde{\alpha}'}}. \quad (26)$$

The force matrix $S_{\tilde{\alpha}\tilde{\alpha}'}$ is precisely the force obtained by Coker and Xiao⁷ using time-dependent perturbation theory applied to the nonlocal Pechukas force.¹⁴ This force acts to redistribute the energy change due to quantum transitions into the classical kinetic energy. The fact that the off-diagonal part of the Liouville super-operator $i\mathcal{L}^Q$ still has a term which involves derivatives with respect to the classical momenta makes the evaluation of the off-diagonal terms difficult. The derivative term can be approximated for small S values as

$$1 + \frac{1}{2} S_{\tilde{\alpha}\tilde{\alpha}'} \cdot \frac{\partial}{\partial P} \approx e^{(1/2) S_{\tilde{\alpha}\tilde{\alpha}'} \cdot \partial / \partial P}, \quad (27)$$

so that accompanying each change in quantum matrix element there is a simultaneous change in momenta whose magnitude and direction are determined by the jump matrix $S_{\alpha\tilde{\alpha}'}$. With this ‘‘momentum-jump’’ approximation, a trajectories method can be developed in which a transition probability matrix is constructed based on $i\mathcal{L}_{\mu\nu}^Q$, resulting in a scheme very similar to that developed by Tully and coworkers.⁴ However, the momentum-jump approximation is quite poor for regions of classical phase space where P is small, or the energy gap is large since the jump matrix $S_{\alpha\tilde{\alpha}'}$ behaves as $M \times (E_{\tilde{\alpha}} - E_{\alpha'})/P$. Transitions in these regions can be cut-off by invoking an *ad-hoc* energy criterion which requires that the classical system has sufficient energy to compensate for a change in the quantum system state.

It is interesting to note that Eq. (22) involves forces that are entirely local in time and instantaneous quantum transitions, unlike many surface-hopping algorithms based on path integral forms of reduced propagators.^{6,7} These properties follow from the application of Trotter’s formula to the mixed quantum-classical Liouville equation. The Trotter formula requires that the time step Δt be small enough so that exponentials of the linear operators $i\mathcal{L}^{cl}$ and $i\mathcal{L}^Q$ commute approximately. The magnitude of the time step Δt between checks for quantum transitions therefore depends on the precise nature of the Liouville operators and is model dependent.

The momentum-jump approximation can be avoided altogether at the expense of introducing additional integrals over singular kernels^{1,2} for *each* derivative with respect to a classical coordinate,

$$\frac{\partial f(R, P)}{\partial P} = - \int_{-\infty}^{\infty} ds \frac{d\delta(s)}{ds} f(P+s). \quad (28)$$

In this scheme, when a transition to another matrix element occurs the actual value of the momentum jump is sampled via a Monte-Carlo procedure from an approximate form of the kernel $d\delta(s)/ds$ for each classical degree of freedom which is coupled to the quantum subsystem. This approach is impractical to implement because the integral over momentum jump values s converges relatively slowly.

The difficulties associated with the evaluation of derivatives with respect to the classical momenta in the off-diagonal coupling matrix can be circumvented by transforming (20) to a basis which diagonalizes the off-diagonal force \mathbf{F} . To accomplish this, we define an R -dependent unitary matrix $\mathbf{U}(R)$ such that (in matrix form)

$$\mathbf{U}^{-1}(R) \cdot \mathbf{F} \cdot \mathbf{U}(R) = \mathbf{F}^d, \quad (29)$$

where \mathbf{F}^d is a diagonal force matrix whose diagonal elements have contributions from the Hellmann–Feynman forces and the off-diagonal force terms. It should be noted that the dimensionality of the transformation matrix $\mathbf{U}(R)$ is the same as that of the *truncated* system of equations in the adiabatic basis. That is, the truncated equation in the adiabatic basis is transformed. As is shown in the Appendix, the equations of motion in matrix form \mathbf{B} for a dynamical variable \hat{B}_w in the *force basis* assume a simple form,

$$\begin{aligned} \frac{d\mathbf{B}(t)}{dt} &= \frac{i}{\hbar} (\tilde{\mathbf{H}}_w \cdot \mathbf{B} - \mathbf{B} \cdot \tilde{\mathbf{H}}_w) + \frac{P}{M} \cdot \frac{\partial \mathbf{B}}{\partial R} \\ &+ \frac{1}{2} \left(\mathbf{F}^d \cdot \frac{\partial \mathbf{B}}{\partial P} + \frac{\partial \mathbf{B}}{\partial P} \cdot \mathbf{F}^d \right), \end{aligned} \quad (30)$$

where

$$\tilde{\mathbf{H}}_w^{\alpha\beta} = H_w^{\alpha\beta} + \frac{i\hbar P}{M} \cdot D^{\alpha\beta}, \quad (31)$$

where α and β are R -dependent force eigenstates and

$$D^{\alpha\beta} = \langle \alpha(R) | \frac{\partial}{\partial R} | \beta(R) \rangle \quad (32)$$

is a nonadiabatic force coupling matrix. Note that since the force matrix \mathbf{F}^d is diagonal in the force basis indices, all coupling between different matrix elements arises solely through the modified commutator term in (30). It should also be noted that for many simple model systems where the coupling between the classical and quantum systems is of the form $V_c(\hat{Q}, \hat{q}) = V(\hat{q})\gamma(\hat{Q})$, the nonadiabatic force coupling matrix \mathbf{D} vanishes.

As in the adiabatic representation, Eq. (30) may be formally solved [in supervector notation with $\mu = (\alpha, \beta)$],

$$\mathbf{B}_w^\mu(t) = (e^{i(\mathcal{L}^Q + \mathcal{L}^{cl})t})_{\mu\nu} \mathbf{B}_w^\nu(0), \quad (33)$$

where $i\mathcal{L}^Q$ is now the off-diagonal commutator term in (30) and $i\mathcal{L}^{cl}$ is a classical-like Liouville operator which is diagonal in the force basis indices,

$$i\mathcal{L}_\mu^{cl} = \frac{P}{M} \cdot \frac{\partial}{\partial R} + \frac{1}{2} \left(\mathbf{F}_{\alpha\alpha}^d \cdot \frac{\partial}{\partial P} + \frac{\partial}{\partial P} \cdot \mathbf{F}_{\beta\beta}^d \right). \quad (34)$$

Since $H_w^{\alpha\beta} = (H_w^{\beta\alpha})^*$ and $D^{\alpha\beta} = -(D^{\beta\alpha})^*$, $i\mathcal{L}^Q$ is an anti-Hermitian operator, as is $i\mathcal{L}^{cl}$. Hence both the off-diagonal Liouville operator $i\mathcal{L}^Q$ and the diagonal operator $i\mathcal{L}^{cl}$ have pure imaginary eigenvalues and satisfy the criteria for the Trotter product formula. Applying the Trotter expansion (21) to Eq. (33), we obtain

$$\begin{aligned} \mathbf{B}_w^\mu(t) &= e^{i\mathcal{L}_\mu^{cl} \Delta t/2} \mathbf{M}_{\mu\nu_1}(\Delta t) e^{i\mathcal{L}_{\nu_1}^{cl} \Delta t/2} \dots e^{i\mathcal{L}_{\nu_N}^{cl} \Delta t/2} \\ &\times \mathbf{M}_{\nu_N \nu}(\Delta t) e^{i\mathcal{L}_\nu^{cl} \Delta t/2} \mathbf{B}_w^\nu(0), \end{aligned} \quad (35)$$

where

$$\mathbf{M}_{\mu\nu}(\Delta t) = [e^{i\mathcal{L}^Q \Delta t}]_{\mu\nu}. \quad (36)$$

The ‘‘transition’’ matrix $\mathbf{M}_{\mu\nu}$ can be explicitly evaluated at any point in classical phase space (R, P) by diagonalizing $i\mathcal{L}^Q$,

$$\mathbf{M}_{\mu\nu}(\Delta t) = \sum_{\hat{\mu}} \mathbf{S}_{\mu\hat{\mu}}(R) e^{i\Omega_{\hat{\mu}}(R, P)\Delta t} \mathbf{S}_{\hat{\mu}\nu}^{-1}(R), \quad (37)$$

where $|\hat{\mu}\rangle$ are the eigenvectors of $i\mathcal{L}^Q$, $\Omega_{\hat{\mu}}(R, P)$ are the corresponding eigenvalues, and $\mathbf{S}(R)$ is the unitary matrix which diagonalizes the $i\mathcal{L}^Q$ matrix written in the force basis set. The ‘‘transition matrix’’ $\mathbf{M}_{\mu\nu}$ is not a transition matrix in the proper sense in that it is not always real, positive with row sums equal to unity. This fact results in numerical insta-

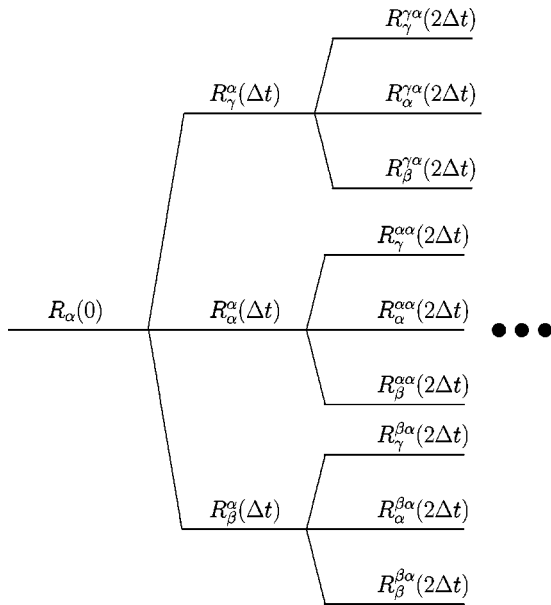


FIG. 1. A schematic representation of the evolution of a super-matrix element R_α for a two-level system starting from time $t=0$. At each time step, there are 3 possible new super-indices possible for the matrix element. The notation $R_\beta^\alpha(\Delta t)$ specifies that the super-index was α and β at times $t=0$ and $t=\Delta t$, respectively.

bilities in the Monte-Carlo procedure we present below, and leads to slow convergence of the method at long times.

For many simple model systems for which the nonadiabatic force coupling matrix vanishes, the adiabatic basis set diagonalizes $i\mathcal{L}^Q$, and the eigenvalues are simply $\Omega_\mu(R) = \omega_{\alpha\beta}(R)$. For these models it is clear that the diagonal terms of the transition matrix are phase terms while couplings among matrix elements occur due to the off-diagonal nature of the partially transformed Wigner Hamiltonian \hat{H}_w in the force basis. In the adiabatic limit, the off-diagonal terms of the force matrix in the adiabatic basis are negligible, in which case the transition matrix is diagonal. For weakly nonadiabatic systems, one can anticipate that the transition matrices have small, complex off-diagonal elements.

III. STOCHASTIC TRAJECTORIES METHOD

From Eq. (35) it is clear that in order to evaluate a particular matrix element $B_w^\nu(t)$ at time t the intermediate force states ν_1, \dots, ν_n must be summed over. For weakly nonadiabatic systems, each sum involves only a few indices. The matrix product in (35) may be viewed as a weighted sum over sets of indices $\{\nu_1, \dots, \nu_n\}$, where the weight of the term is determined by the product of the matrix elements at each time-step. If there are M indices referring to the quantum matrix elements in the truncated system of equations then there are clearly M^{N_i} sets of indices. As the quantum forces in each quantum state are potentially different, there are therefore also on the order of M^{N_i} distinct classical ‘‘paths’’ for the bath degrees of freedom since the value of the classical phase space coordinates at each time increment depends on the *entire* history of the path preceding it. A schematic representation of the series is shown in Fig. 1. However, not all paths contribute to the dynamics of a par-

ticular matrix element with equal weight, and importance sampling can be used to approximate the sum over all possible sets of indices. The actual way in which the sampling is done is arbitrary, provided the sampling method converges to the correct result.

The method can be illustrated by considering a simple problem of calculating a product of nearly-diagonal, complex matrices by a Monte-Carlo procedure,

$$M^{\alpha\beta} = \sum_{\gamma_1, \dots, \gamma_n} M_1^{\alpha\gamma_1} M_2^{\gamma_1\gamma_2} \dots M_{n-1}^{\gamma_{n-1}\beta} \quad (38)$$

$$= \sum_{\gamma_1, \dots, \gamma_n} \frac{M_1^{\alpha\gamma_1}}{P_1(\alpha, \gamma_1)} \frac{M_2^{\gamma_1\gamma_2}}{P_2(\gamma_1, \gamma_2)} \dots \frac{M_{n-1}^{\gamma_{n-1}\beta}}{P_{n-1}(\gamma_{n-1}, \beta)} \times P_1(\alpha, \gamma_1) \dots P_{n-1}(\gamma_{n-1}, \beta), \quad (39)$$

where $P_i(\alpha, \beta)$ is the conditional probability of choosing index β given that the current index is α for matrix i . One reasonable choice of how $P_i(\alpha, \beta)$ can be defined is

$$P_i(\alpha, \beta) = \frac{|M_i^{\alpha\beta}|}{\sum_\gamma |M_i^{\alpha\gamma}|}, \quad (40)$$

where $|M^{\alpha\beta}|$ is the modulus of complex matrix element $M^{\alpha\beta}$. The Monte-Carlo procedure is to first construct the probability distribution $P_i(\gamma_{i-1}, \gamma_i)$ given that the current index is γ_{i-1} , and then to draw the index γ_i randomly from the constructed distribution P_i . After drawing the indices, the weight factor for each Monte-Carlo sampling step is calculated as $M_i^{\gamma_{i-1}\gamma_i}/P_i(\gamma_{i-1}, \gamma_i)$. The process is continued sequentially for $i=1$ to $i=n-1$. The cumulative ‘‘Rosenbluth’’¹⁷ weight factor for the entire process is the product of each of the individual step weight factors, much as in configurational biased sampling.¹⁸ The estimator for $M^{\alpha\beta}$ is computed by averaging over a large number of realizations of this procedure. If the matrices M_i have small off-diagonal elements, the Monte-Carlo procedure will converge quickly to $M^{\alpha\beta}$.

The Monte-Carlo procedure elaborated above is clearly not the most efficient way of evaluating the matrix product. However, the scheme can be also be applied in the case in which the M_i depend on all previous matrices M_j with $j < i$. In this situation the P_i are distributions which depend on the entire previous history of indices selected. This is clearly the case for the mixed quantum-classical evolution.

The exact surface-hopping algorithm for performing mixed quantum-classical molecular dynamics to calculate a specific matrix element $B_w^\mu(t)$ at time t is therefore the following.

- (1) Given the current (or initial) values of R and P , solve the instantaneous eigenvalue equation to calculate the adiabatic states and the force matrix \mathbf{F} in the adiabatic basis.
- (2) Find the unitary transformation matrix $\mathbf{U}(R)$ that diagonalizes \mathbf{F} and calculate the new diagonal force matrix \mathbf{F}_d .

- (3) Given the current (or initial) matrix index ν_i , propagate, using the force $\mathbf{F}_{\nu_i}^d$, the classical coordinates using a reversible molecular dynamics procedure, like leapfrog, for a short time interval $\Delta t/2$.
- (4) Construct the adiabatic and force states at the new classical coordinates and diagonalize the off-diagonal Liouville operator $i\mathcal{L}^Q$ to form the transition matrix \mathbf{M}_i using Eq. (37).
- (5) Construct a probability distribution function $P_i(\nu_i, \nu_{i+1})$ based on \mathbf{M}_i and select a force state ν_{i+1} from P_i . Calculate the weight factor \mathbf{M}_i/P_i .
- (6) Repeat steps (1)–(3) with the index ν_{i+1} .
- (7) Repeat steps 1 through 6 N_i times and calculate the cumulative weight factor by multiplying together the weight factors from each iteration. Calculate B_w at the final classical coordinate values and multiply by the weight factor.
- (8) Repeat the entire procedure, steps (1)–(7), N_{mc} times and average to obtain an estimate of $B_w^\mu(t)$.

The algorithm requires solving for the instantaneous adiabatic and force states 3 times per time step. The additional force state diagonalization not present in other methods introduces little additional work since the force matrix in the (truncated) adiabatic basis is typically of low dimension for weakly nonadiabatic systems. Similar considerations hold for the diagonalization of $i\mathcal{L}^Q$.

IV. RESULTS ON A MODEL SYSTEM

The new surface-hopping method was tested on a simple one-dimensional model system comprised of a quantum double-well system bilinearly coupled to a Harmonic oscillator bath. A similar system was used by Fang and Hammes-Schiffer¹⁹ to study the ‘‘fewest switches’’ stochastic algorithm. The partially-Wigner transformed Hamiltonian for the model system is

$$\hat{H}_w = \frac{\hat{p}^2}{2m} + 0.25c_0\hat{q}^4 - 0.5a_0\hat{q}^2 - \gamma\hat{q}R + \frac{P^2}{2M} + \frac{1}{2}\hbar M\omega_0^2 R^2, \quad (41)$$

where $m=1$ amu, $M=100$ amu, $a_0=565 \text{ \AA}^{-2}$ kcal/mol, $c_0=9975 \text{ \AA}^{-4}$ kcal/mol, $\gamma=63.33 \text{ \AA}^{-2}$ kcal/mol, and $\omega_0=100 \text{ cm}^{-1}$. These parameter values give a double-well barrier height of 8 kcal/mol at $\pm 0.24 \text{ \AA}$ and yield a frequency typical of an OH stretching vibration.¹⁹ It is convenient to introduce dimensionless scaled variables defined by

$$t = \omega_0^{-1} t^*, \quad P = (M\hbar\omega_0)^{1/2} P^*, \quad (42)$$

$$R = \left(\frac{\hbar}{M\omega_0} \right)^{1/2} R^*, \quad \gamma = \omega_0(M\hbar\omega_0)^{1/2} \gamma^*,$$

and energy is expressed in units of $\hbar\omega_0$. In Fig. 2, the adiabatic potential energy curves, and the nonadiabatic coupling element d_{12} are shown as a function of dimensionless classical coordinate R^* . The model has an avoided crossing in the vicinity of $R^*=0$ where the nonadiabatic coupling matrix has a maximum. In this region of the classical phase space, the adiabatic surfaces are coupled and a significant

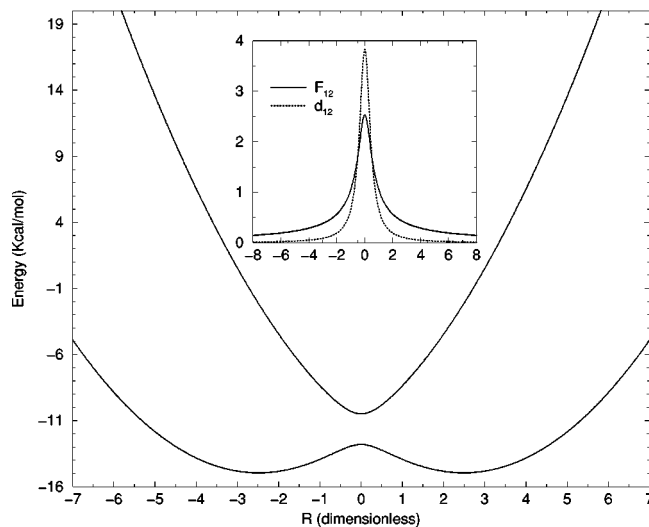


FIG. 2. The adiabatic energy levels and off-diagonal force and coupling matrix for the model proton transfer system as a function of reduced spatial coordinate R .

redistribution of population occurs as the classical system evolves. Note that d_{12} is a long-ranged function of R which decays to zero as R^{-2} for large R in this model, while the off-diagonal force decays as R^{-1} . The long-ranged nature of these matrix elements implies that the coupling between adiabatic surfaces extends over a wide region of classical phase space.

It is straightforward to show that the correction terms for higher orders of the small expansion parameter ϵ vanish for a classical Harmonic oscillator bilinearly coupled to a quantum subsystem due to the fact that the higher order terms introduce higher order derivatives, via the Poisson bracket operator, which vanish or cancel for the simple model system. The mixed quantum-classical Liouville equation (4) is therefore *exact* for this model. This implies the Monte-Carlo method proposed in the preceding section converges to the exact quantum result regardless of the ratio of the classical and quantum masses in the Hamiltonian (41). The importance of higher order terms in (4) for other models remains to be examined.

A. Fourier-transform solution

Equation (35) can be solved numerically to arbitrary accuracy using finite grid methods. In this approach, the set of matrices $\mathbf{B}_w^\mu(R_i, P_i)$ is embedded on a finite grid that spans the phase space, where the index i runs over the grid points. The number of grid points and their distribution are optimized to achieve the desired level of accuracy as function of computational cost. For an infinitesimal time interval Δt , the quantum propagation corresponds to a matrix rotation based on Eq. (36). For the propagation with the classical propagator $i\mathcal{L}^{\text{cl}}$, we need to make a transformation to the appropriate reciprocal space of R and P such that the operators $\partial/\partial R$ and $\partial/\partial P$ become diagonal. This procedure can easily be implemented with the fast-Fourier-transform (FFT) package.

The FFT method is intrinsically a rigorous method. The drawback of it is that it becomes computationally costly as soon as one turns to systems of higher dimensionality, which renders the method impractical for systems with many degrees of freedom. However, the FFT method does give us good reference solutions against which the solutions obtained by stochastic methods for the model systems may be tested.

B. Surface-hopping solution

In order to implement the surface-hopping method outlined in Sec. III for the model system, the sampling procedure must be specified by defining the distribution $P(\alpha, \beta)$. Based on the example (39), the logical choice of distribution is

$$P(\mu, \nu) = \frac{|M_{\mu\nu}|^\theta}{\sum_\gamma |M^{\mu\gamma}|^\theta}, \quad (43)$$

where $\theta=1$, μ and ν are *super-vector* indices, and $M_{\mu\nu}$ is the transition matrix (37). It is possible that other values of θ and other forms of the sampling distribution allow for faster convergence of the Monte-Carlo procedure. Because the nonadiabatic force coupling matrix $D=0$ for this model, the construction of the sampling distribution $P(\mu, \nu)$ is straightforward and introduces little computational work beyond the construction of the instantaneous adiabatic and force states. Based on the observation that the population of the second excited state (and higher states) obtained from the exact fast Fourier transform solution of (30) is negligible for the coupling value $\gamma=63.33 \text{ \AA}^{-2} \text{ kcal/mol}$, the adiabatic states are truncated to include only two states and the model is essentially a two-level quantum system bilinearly coupled to a classical harmonic oscillator. In the trajectory calculations presented here, the adiabatic states are calculated by first diagonalizing the quantum double-well Hamiltonian terms (without the coupling to the bath) very accurately using an essentially complete Hermite basis set for the \hat{q} operator. Once the ‘‘subsystem’’ states are obtained, the partially Wigner-transformed Hamiltonian \hat{H}_w is written in the subsystem basis. The adiabatic basis states at each classical R value are then obtained by diagonalizing the \hat{H}_w matrix. The initial step of solving for the subsystem states is independent of R and therefore needs to be done only once. The subsystem states are useful because accurate calculation of the lowest adiabatic eigenstates (and eigenvalues) requires relatively few subsystem states for systems which are localized in regions of classical phase space near $R=0$. Typically, between 2 to 8 subsystem states are necessary for converged adiabatic energies and forces, depending on the coupling strength γ . Several observables were calculated via the stochastic molecular dynamics procedure, $R(t)$, $P(t)$, $R^2(t)$, $P^2(t)$, the total energy, $E(t)$, and the ground and excited adiabatic state populations. In Fig. 3, results of the stochastic algorithm are compared to the exact solution obtained using the Fourier transform method. The trajectories and populations obtained using the MDQT method⁴ of Tully and

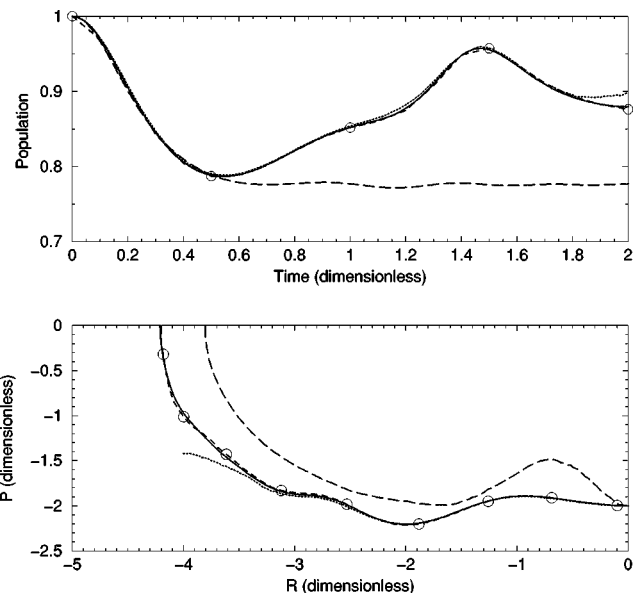


FIG. 3. The populations and phase-space trajectory for the model proton transfer system. The solid lines indicate the exact numerical solution obtained by FFT methods, the long-dashed line are the MDQT results, the dotted line are the exact surface-hopping results, and the dashed-line labeled with circles are the results from the ‘‘localized thread’’ algorithm described in Sec. V.

Hammes-Schiffer are also included in Fig. 3 for comparison. As the Fourier transform method requires a distribution of initial conditions with finite width, the classical trajectories and adiabatic state populations were calculated from a set of 100 initial points for R and P drawn from a narrow Gaussian,

$$\frac{w}{\pi} e^{-w(R-R_0)^2} e^{-w(P-P_0)^2}, \quad (44)$$

of width $w=50$ centered at $R_0=0$ and $P_0=-2$. The quantum system was assumed to be initially in the ground adiabatic state. The adiabatic population for quantum state $\tilde{\mu}$ was calculated by evolving the variable $\delta(R-R_0)\delta(P-P_0)\delta_{\tilde{\mu},\nu}$ for each set of initial classical coordinates. The trajectory and populations for each initial point was averaged over $N_{mc}=50\,000$ sampling trajectories. As is evident in Fig. 3, the Monte-Carlo sampling procedure does indeed converge to the exact quantum result, although the convergence rate is disappointing and many trajectories must be sampled. Although total energy and population are conserved explicitly in (30), these quantities vary along each of the sampling trajectories and are conserved only in the final converged average over all the sampling trajectories. They therefore can be used to monitor the convergence of the Monte-Carlo sampling procedure. In Fig. 4, the total energy and population are plotted as a function of time, from which it is evident that although the short-time dynamics (from $\omega_0 t < 1$) conserves the energy and total population on average, significant deviations due to statistical fluctuations of the average energy and total populations appear at longer times. The errors in conservation of the energy and total population are correlated due to the way in which the trajectories are weighted. To further investigate this behavior, the average classical R and P trajectories through the nonadiabatic region, along with the

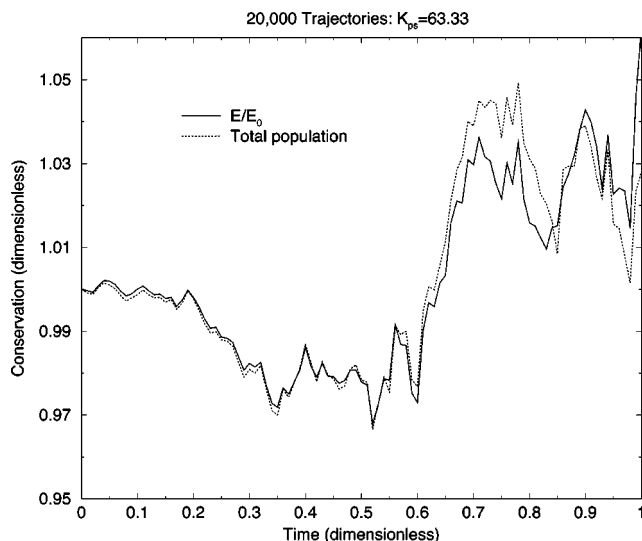


FIG. 4. The energy conservation of the exact surface-hopping trajectory method. The deviations are due to the stochastic nature of the method.

statistical uncertainties of these averages, estimated using 200 bootstrap samples,²⁰ were calculated and plotted as a function of time in Fig. 5. The averages were calculated from 20,000 sampling trajectories which all started from the initial condition $R=0$, $P=-2$. It is clear from Fig. 5 that the growth in the statistical uncertainty is exponential in time, so the method is impracticable for calculating long molecular dynamics trajectories for this model.

The instability of the sampling procedure can be understood by close examination of the behavior of the transition matrix $M_{\mu\nu}$ as a function of the R coordinate. Ideally, one hopes the off-diagonal elements $M_{\mu\nu}$ are significant only in the nonadiabatic region of phase space so that as the system moves away from the system it makes fewer and fewer transitions. This property arises naturally when the dynamics of the system is expressed in the adiabatic basis. In the force basis, however, even though the transition matrix is nearly

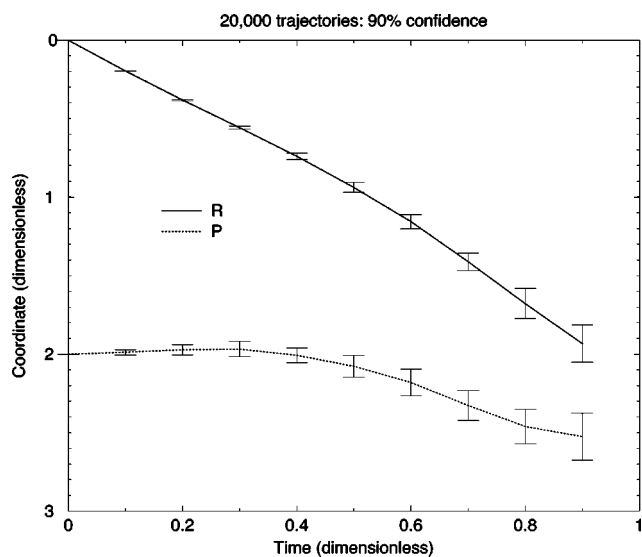


FIG. 5. Growth of the uncertainties of the average classical trajectory coordinates calculated by the surface-hopping method as a function of time.

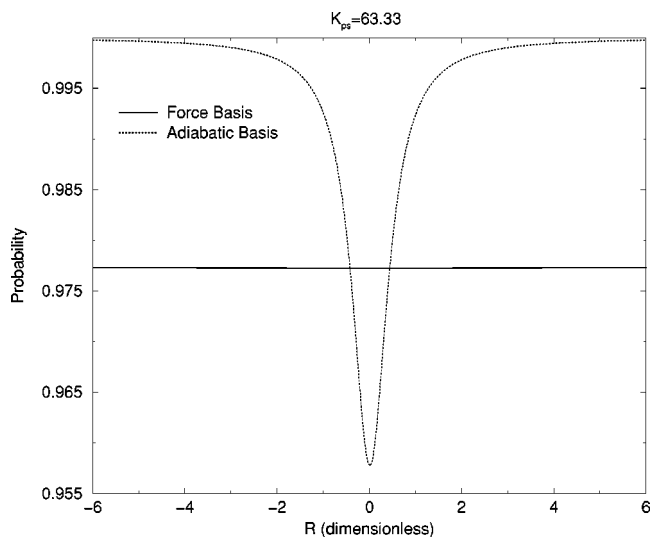


FIG. 6. The probability of making a transition from the ground state in the adiabatic and force basis representation of the quantum subsystem.

always diagonal it is relatively *constant* over the entire region of phase space, as is seen in Fig. 6, so that the natural evolution of the system does not cut-off the transitions. The transitions in the force basis are effectively distributed evenly in time, leading to an accumulation of uncertainty at longer times. The accumulation is due to the fact that since the transition matrix $M_{\mu\nu}$ is not a transition matrix in the proper sense, the cumulative Rosenbluth weight grows in time since the weight at each time-step is proportional to $Q^\mu = \sum_\gamma |M_{\mu\gamma}|^\theta$. For the bilinear coupling model, $Q^\mu > 1$ and is a constant which depends on the coupling strength parameter γ . This, in turn, implies that the range of the “weights” for the sampling trajectories grows as time increases, resulting in numerical instabilities associated with averaging over a broad (and multi-modal) distribution of trajectories. The instability is compounded by the fact that the “weights” in the ensemble of sampling trajectories are both positive and negative, which ideally nearly cancel one another. The poor convergence of the stochastic algorithm due to the contribution of different signs is similar to the one usually encountered in semi-classical methods like the IVR.¹² However, the signs flips occur in the transition matrices in a regular way, and it seems likely that the convergence of the method would be vastly improved if the symmetries which lead to the near cancellations in contributions to averages of observables were incorporated into the sampling procedure.

However, there are positive aspects of the Monte-Carlo method. The sampling procedure converges reasonably well for short-time dynamics *regardless* of whether the region of classical phase space is nonadiabatic or not. In instances in which only the short-time dynamics is of interest, such as in the estimation of rate constants for chemical processes,²¹ the method is potentially useful. Furthermore, it is possible that the qualitative nature of the transition matrix will be substantially different in models where the nonadiabatic coupling matrix and off-diagonal forces are localized in specific regions of phase space, leading to natural transition cut-offs in

the force basis as well. These issues are currently under investigation.

The unpleasant properties of the transition matrix $M_{\mu\nu}$ are a reflection of the fact that the force basis is not the ‘‘natural’’ basis for the weakly nonadiabatic dynamics, and it is logical to try to apply a methodology similar to that used in developing the force basis surface-hopping algorithm to dynamical equations written in the adiabatic basis. Unfortunately, such an approach is difficult to implement due to even worse sampling instabilities. For example, an exact Monte-Carlo procedure based on (22) can be devised in which transitions among adiabatic matrix elements are sampled from a distribution. Consider the resulting transition matrix,

$$M_{\mu\nu}^{\tilde{\nu}}(\Delta t) = (e^{i\tilde{\mathcal{L}}_1 \Delta t})_{\mu\nu}^{\tilde{\nu}}. \quad (45)$$

As in (37), the off-diagonal Liouville operator (now in the adiabatic basis) can be written as

$$M_{\mu\nu}^{\text{ad}}(\Delta t) = \sum_{\hat{\mu}} \mathbf{S}_{\hat{\mu}\hat{\mu}}^{\text{ad}}(R) e^{i\tilde{\mathcal{L}}_{\hat{\mu}}(R,P)\Delta t} \mathbf{S}_{\hat{\mu}\nu}^{-1}(R), \quad (46)$$

where $\hat{\mu}$ is the basis set which diagonalizes the super-matrix $i\tilde{\mathcal{L}}_1$ and $\tilde{\mathcal{L}}_{\hat{\mu}}$ is the resulting linear operator which is now diagonal in quantum super-indices. As is apparent from Eq. (15), $\tilde{\mathcal{L}}_{\hat{\mu}}$ contains a term of the form $\tilde{\mathbf{F}}_{\hat{\mu}} \cdot \partial/\partial P$, which provides a natural momentum jump whose magnitude is dictated by $\tilde{\mathbf{F}}_{\hat{\mu}}$. Considering only the term in $\tilde{\mathcal{L}}_{\hat{\mu}}$ due to the off-diagonal force, the transition matrix can be explicitly evaluated by adding a well-defined momentum jump at every time-step. However since each intermediate state $\hat{\mu}$ gives a different momentum jump, the intermediate state must be sampled by some procedure in addition to the adiabatic state in order to uniquely specify the subsequent classical trajectory. This can be implemented by writing

$$M_{\mu\nu}^{\text{ad}}(\Delta t) = \sum_{\hat{\mu}} M_{\mu\nu}^{\text{ad}}(\hat{\mu}, \Delta t) \quad (47)$$

$$= \sum_{\hat{\mu}} \frac{M_{\mu\nu}^{\text{ad}}(\hat{\mu}, \Delta t)}{P_{\hat{\mu}\nu} P(\hat{\mu}|\tilde{\mu}\tilde{\nu})} P_{\mu\nu} P(\hat{\mu}|\tilde{\mu}\tilde{\nu}) \quad (48)$$

$$= \sum_{\hat{\mu}} W(\hat{\mu}, \tilde{\mu}, \tilde{\nu}) P_{\mu\nu} P(\hat{\mu}|\tilde{\mu}\tilde{\nu}), \quad (49)$$

where $P(\tilde{\mu}, \tilde{\nu})$ is the probability of choosing adiabatic state $\tilde{\nu}$ given that the system is in state $\tilde{\mu}$, $P(\hat{\mu}|\tilde{\mu}\tilde{\nu})$ is the conditional probability of selecting intermediate state $\hat{\mu}$ given adiabatic states $\tilde{\mu}$ and $\tilde{\nu}$, and $W(\hat{\mu}, \tilde{\mu}, \tilde{\nu})$ is the weight factor for selecting $\hat{\mu}$ and $\tilde{\nu}$ given $\tilde{\mu}$. The obvious choice of the sampling distributions is

$$P(\hat{\mu}|\tilde{\mu}\tilde{\nu}) = \frac{|M_{\mu\nu}^{\text{ad}}(\hat{\mu}, \Delta t)|}{\tilde{Q}_{\mu\nu}^{\tilde{\nu}}},$$

$$P_{\mu\nu}^{\tilde{\nu}} = \frac{Q_{\mu\nu}^{\tilde{\nu}}}{\sum_{\gamma} Q_{\mu\gamma}^{\tilde{\nu}}}, \quad (50)$$

with

$$Q_{\mu\nu}^{\tilde{\nu}} = \left| \sum_{\hat{\mu}} M_{\mu\nu}^{\text{ad}}(\hat{\mu}, \Delta t) \right|, \quad (51)$$

$$\tilde{Q}_{\mu\nu}^{\tilde{\nu}} = \sum_{\hat{\mu}} |M_{\mu\nu}^{\text{ad}}(\hat{\mu}, \Delta t)|. \quad (52)$$

At first glance one might think the method is useful since the transition probability now reflects the true nature of the weakly nonadiabatic system. However, when rare transitions among adiabatic matrix elements occurs in regions where $Q_{\mu\nu}^{\tilde{\nu}} < 0$ for $\tilde{\nu} \neq \tilde{\mu}$ (and hence $P_{\mu\nu}^{\tilde{\nu}} < 1$), the weight factor $W(\hat{\mu}, \tilde{\mu}, \tilde{\nu})$ becomes large since it is proportional to the ratio $\tilde{Q}_{\mu\nu}^{\tilde{\nu}}/Q_{\mu\nu}^{\tilde{\nu}}$ and $\tilde{Q}_{\mu\nu}^{\tilde{\nu}} \sim 1$. The divergent weight factor causes far greater instabilities than those encountered in the force basis method. The only way in which the sum over intermediate states $\hat{\mu}$ can be done explicitly to avoid the additional sampling is if the transition matrix M does not alter the classical trajectory. This requires a diagonal force, and one is reduced to the force basis representation if the surface-hopping is to be done exactly.

V. AN ASYMPTOTIC SOLUTION METHOD FOR THE MIXED QUANTUM-CLASSICAL LIOUVILLE EQUATION

A. Formulation

In this section we focus on a new deterministic method of solving the mixed quantum-classical Liouville equation that remains computationally practical, and through which the question of numerical accuracy can be addressed on a fundamental level. The method is based upon the notion of locality in classical phase space of classical trajectories.

Consider the partially Wigner transformed density matrix $\hat{\rho}_w(R, P, t)$, where R and P are the multi-dimensional phase space coordinates for the classical degrees of freedom. There is one to one correspondence between the matrix element $\rho_w^{\alpha\beta} = \langle \alpha | \hat{\rho}_w | \beta \rangle$ and the true quantum density matrix $\rho_Q = |\alpha\rangle\langle\beta|$. Our fundamental assumption is that for the time intervals which are of physical interest, $\hat{\rho}_w$ is localized within a finite volume Ω of classical phase space, over which its matrix elements represented in a quantum basis are relatively smooth. Under these conditions, a finite number of matrices located at a set of discrete points in classical phase space, $\{\hat{\rho}_w^j(R_j, P_j, t)\}$, $j=1, 2, \dots, L$, can be found which can approximately represent the exact density matrix to any desired accuracy when L is sufficiently large;

$$\hat{\rho}_w(R, P, t) = \sum_{j=1}^L \hat{\rho}_w^j(t) \delta(R - R_j(t)) \delta(P - P_j(t)). \quad (53)$$

Inserting the finite representation of $\hat{\rho}_w$ in (53) into the Liouville equation (7) yields

$$\sum_{j=1}^L \frac{\partial}{\partial t} [\hat{\rho}^j(t) \delta(R-R_j) \delta(P-P_j)] \\ = \sum_{j=1}^L (i\mathcal{L}^Q + i\mathcal{L}^R + i\mathcal{L}^P) \hat{\rho}^j \delta(R-R_j) \delta(P-P_j), \quad (54)$$

where $i\mathcal{L}^Q$ is the quantum part the Liouville operator, and $i\mathcal{L}^R$ and $i\mathcal{L}^P$ are the classical parts that act on R and P , respectively. We can subsequently break the above equation into three coupled equations:

$$\frac{\partial}{\partial t} \hat{\rho}^j(t) = i\mathcal{L}^Q(R_j, P_j) \hat{\rho}^j(t), \quad (55)$$

$$\frac{\partial}{\partial t} \delta(R-R_j) = i\mathcal{L}^R(R_j, P_j) \delta(R-R_j), \quad (56)$$

$$\hat{\rho}^j \frac{\partial}{\partial t} \delta(P-P_j) = i\mathcal{L}^P(R_j, P_j) \hat{\rho}^j \delta(P-P_j). \quad (57)$$

Notice we have utilized the property that $i\mathcal{L}^R$ and $\hat{\rho}$ commute, so the density matrix does not explicitly appear in Eq. (56).

Equations (55)–(57) can be compared to the case where the quantum density evolution is superposed on a set of point particles that evolves classically according to the Liouville equation. The latter can be solved numerically via a simple leap-frog type procedure. The major difference here is that the operator $i\mathcal{L}^P$ does not commute with $\hat{\rho}$, and we need to have a closer look at Eq. (57), which we express as

$$\hat{\rho}^j \frac{\partial}{\partial t} \delta(P-P_j) \\ = -\frac{1}{2} [\hat{\mathbf{F}}_w(R_j) \hat{\rho}^j + \hat{\rho}^j \hat{\mathbf{F}}_w(R_j)] \cdot \frac{\partial}{\partial P} \delta(P-P_j), \quad (58)$$

where $\hat{\mathbf{F}}_w$ is the mixed quantum-classical force operator. To obtain (58), we have assumed that $\hat{\mathbf{F}}_w$ is independent of P . The development of the dynamical equations (55)–(57) is general and independent of the basis set used to represent the quantum operators. Usually the quantum basis set is chosen with a cut-off in energy and has a finite dimension M to take advantage of the fact that only a few adiabatic energy states have significant population. In this truncated quantum basis representation, $\hat{\mathbf{F}}_w$ and $\hat{\rho}$ are $M \times M$ matrices. The quantum basis typically depends parametrically on the classical coordinate R , which affects the form of the subsequent evolution equations. For example, consider a generic local basis set [parametrically dependent on the classical coordinate R], $|\phi_\alpha(R)\rangle$, $\alpha = 1, 2, \dots, M$, in which the operators in Eqs. (57) are represented as matrices. Care must be taken when evaluating the equations of motion for the matrix elements using (55)–(57) due to the explicit R dependence in the basis set. The left hand side of the equation (55) involves a derivative with respect to time on the operator $\hat{\rho}$. Since the classical coordinates depend implicitly on time, the left hand side of (55) becomes

$$\langle \alpha | \frac{\partial}{\partial t} \hat{\rho} | \beta \rangle = \frac{\partial}{\partial t} \rho_{\alpha\beta} - \rho_{\alpha\gamma} \mathbf{d}_{\gamma\beta} \cdot \frac{P}{M} + \frac{P}{M} \cdot \mathbf{d}_{\alpha\gamma} \rho_{\gamma\beta}, \quad (59)$$

where we have inserted the relation $\langle \alpha | \partial_t | \beta \rangle = (P/M) \times \langle \alpha | \nabla_R | \beta \rangle \equiv (P/M) \mathbf{d}_{\alpha\beta}$. In the R -dependent basis set, the equations of motion for the matrix elements and their classical coordinates are

$$\frac{\partial}{\partial t} \rho_{\alpha\beta}^j(t) = i\mathcal{L}_{\alpha\beta, \alpha'\beta'}^Q(R_j, P_j) \rho_{\alpha'\beta'}^j(t), \quad (60)$$

$$\frac{\partial}{\partial t} \delta(R-R_j) = i\mathcal{L}^R(R_j, P_j) \delta(R-R_j), \quad (61)$$

$$\rho_{\alpha\beta}^j \frac{\partial}{\partial t} \delta(P-P_j) = i\mathcal{L}_{\alpha\beta, \alpha'\beta'}^P(R_j, P_j) \rho_{\alpha'\beta'}^j \delta(P-P_j), \quad (62)$$

where the terms involving the d matrix have been incorporated into the right hand side of (60) as part of the quantum Liouville operator $i\mathcal{L}^Q$. The Liouville operators can be explicitly written out in the basis representation as

$$i\mathcal{L}_{\alpha\beta, \alpha'\beta'}^Q \rho_{\alpha'\beta'} = -\frac{i}{\hbar} H_w^{\alpha\gamma} \rho_{\gamma\beta} + \frac{i}{\hbar} \rho_{\alpha\gamma} H_w^{\gamma\beta} - \frac{P}{M} \\ \cdot \mathbf{d}_{\alpha\gamma} \rho_{\gamma\beta} + \rho_{\alpha\gamma} \mathbf{d}_{\gamma\beta} \cdot \frac{P}{M}, \quad (63)$$

and

$$i\mathcal{L}_{\alpha\beta, \alpha'\beta'}^P \rho_{\alpha'\beta'} = -\frac{1}{2} (\hat{\mathbf{F}}_w^{\alpha\gamma} \rho_{\gamma\beta} + \rho_{\alpha\gamma} \hat{\mathbf{F}}_w^{\gamma\beta}) \cdot \frac{\partial}{\partial P}. \quad (64)$$

The quantum basis we propose is a basis that diagonalizes the force operator so that $\hat{\mathbf{F}}_w^{\alpha\beta} = \mathbf{f}_\alpha \delta_{\alpha\beta}$, and Eq. (62) becomes

$$\left(\frac{\partial}{\partial t} \right)_{\alpha\beta} \delta(P-P_j) = -\frac{1}{2} [\mathbf{f}_\alpha(R_j) + \mathbf{f}_\beta(R_j)] \cdot \frac{\partial}{\partial P} \delta(P-P_j), \quad (65)$$

where \mathbf{f}_α is the eigenvalue of the force matrix (i.e., $\hat{\mathbf{F}}_w |\alpha\rangle = \mathbf{f}_\alpha |\alpha\rangle$). The indices on the left hand side of (65) indicate that the classical coordinate P_j of matrix element $\rho_{\alpha\beta}^j$ is evolving according to the force corresponding to indices $(\alpha\beta)$. It is readily apparent that different matrix elements will propagate according to different quantum forces, leading to a branching of classical trajectories for each matrix element.

The branching effect greatly complicates the solution of the dynamical evolution equations. For example, suppose that at a given time a discrete set of density matrices is found to represent the density matrix to some desired accuracy. According to Eqs. (60)–(62) and (65), each matrix in this set will branch into $M(M+1)/2$ matrices due to the off-diagonal nature of $i\mathcal{L}^Q$ in the basis set in the next small time interval. The total number of matrices we get after such an iteration will be $L \times M(M+1)/2$. According to the fundamental assumption of localization in classical phase space, there must be L among those that will best represent the total density at time $t + \Delta t$. The primary task in our algorithm is to find L matrices from among the total number $L \times M(M+1)/2$ after each iteration that can best represent the quantum density matrix. We propose the following rules for this purpose: (1) We define the weight of each matrix to be $\sum_{\alpha\beta} |\rho_{\alpha\beta}|$. If this weight is less than a certain small number, such as 10^{-12} , then this thread ‘‘dies’’ and is dropped from

the set. (2) If two threads are close to each other, namely, if their distance in phase space is less than a small critical number, then these two threads are simply superposed to form one thread. By applying the above two rules, the total number of threads can be reduced in a well-controlled manner. As we will show in the next section, the results of this asymptotic approach agree very well with the exact solutions for the test model we have studied.

Recently, Martínez and coworkers have developed a multiple spawning (MS) numerical scheme for the study of nonadiabatic dynamics.²² Essentially, the MS method uses a moving Gaussian basis set to expand the wavefunction of the heavy particles. Each Gaussian state is centered along a classical trajectory whose time evolution is determined by the potential of the corresponding (quantum) energy surface of the light particles (electron). Gaussians of different energy surfaces are coupled through nonadiabatic interaction terms. Usually this method starts with a minimum set of basis functions, and the basis set is expanded and new functions are ‘spawned’ to describe nonadiabatic events occurring in the crossing region.

Although both the MS and the present method use the spawning scheme, the former spawns new basis elements and the latter spawns new threads. The two methods are fundamentally different. The MS method is essentially a full quantum solution in nature, with a sufficiently large basis set cleverly placed to describe the full system quantum mechanically. The present method, however, is based on a mixed quantum and classical equation where the degrees of freedom of the heavy particles are treated classically. The partially Wigner-transformed density matrix, which is the fundamental quantity considered here, is equivalent to the true quantum density matrix in the limit that the degrees of freedom of the heavy particles are propagated using semiclassical schemes such as the WKB method.²³

There is also an important difference between the two methods on a practical level. In the localized-thread method, creating and combining threads do not require the time-consuming calculation of the Hamiltonian and overlap matrices of basis elements. For this reason, we expect the localized-threads algorithm to be much less computationally demanding than other spawning methods.

B. Performance on the model system

The ‘localized-threads’ algorithm outlined above was tested on the model system of the previous section. As in the MDQT scheme,⁴ the 100 initial phase space points were sampled from the distribution (44). The maximum number of threads L was set to be 500 and the distance cut-off in phase space was allowed to grow in order to maintain at most the maximum number of threads (i.e., the number of threads L was held fixed by combining as many threads as necessary). The results of the localized threads algorithm are shown in Fig. 3 along with the exact (FFT), exact surface-hopping, and MDQT results. It is evident in Fig. 3 that the localized threads algorithm works quite well for the model system with $L=500$, with an accuracy comparable to that of the exact surface-hopping algorithm in an order of magnitude less computational time. The method calculates the entire

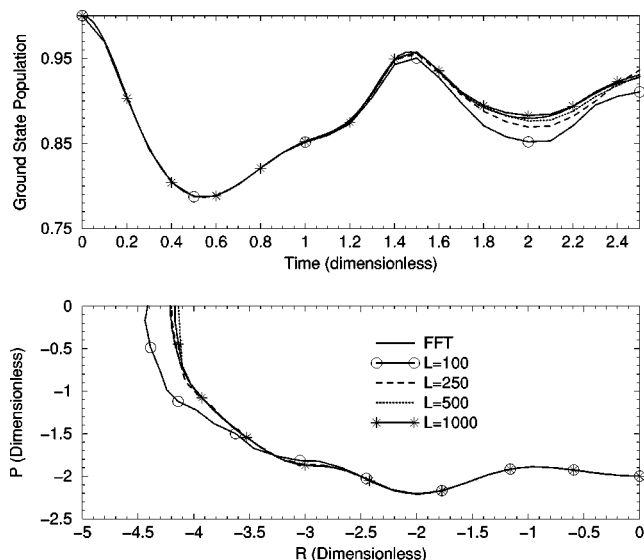


FIG. 7. Convergence behavior of the localized thread algorithm as a function of the maximum number of threads L . All threads started in the ground adiabatic energy state with classical coordinates $R=0$ and $P=-2$.

phase space trajectory almost exactly over the entire time range and gives the correct classical turning point. The deviations observed in the populations at longer times (around $\omega_0 t = 2$) can be reduced in a well-controlled fashion by systematically increasing L until convergent results are obtained. In Fig. 7 the populations and phase space trajectories as a function of the maximum number of threads is plotted. All the threads started from the same initial phase space point $R=0.0$, $P=-2.0$. It is remarkable that as few as 250 threads can be used to obtain trajectories and populations with an accuracy of several percent for time-scales long enough to reach the turning point, even at relatively low kinetic energies.

The computational cost of the localized thread algorithm with maximum threads L corresponds to utilizing approximately $3L$ trajectories in the MDQT algorithm for the model system. Although the MDQT method works well for initial conditions of high kinetic energy, the MDQT method performs quite poorly for the (low energy) parameters we have chosen compared to the exact result primarily due to a neglect of classical forbidden transitions. These transitions play an important role in de-populating the excited state in regions of non-negligible nonadiabatic coupling and relatively large energy gaps. The localized threads algorithm does not rely upon any *ad-hoc* rules of energy conservation and reproduces the correct populations very well. One of the useful features of many surface-hopping algorithms is the facility of implementing them on parallel computer platforms. We note that the implementation of a parallel localized threads algorithm is straightforward by first drawing a large collection of initial conditions and then forming groups of threads to be propagated on separate computational nodes.

VI. SUMMARY AND CONCLUSIONS

In this article we have presented two possible practical methods of solving the mixed quantum-classical Liouville

equation. The first technique is a stochastic surface-hopping method which converges to the exact result as the number of sampling trajectories increases. Unfortunately, the sampling method outlined here is inherently unstable because the “transition matrix” $M^{\mu\nu}$ is not a proper transition matrix. It is possible that a different sampling procedure which takes advantage of system symmetries would ameliorate the rate of convergence of the method. In its current form, the exact surface hopping method is suitable for calculating dynamical properties on short time-scales. It remains to be seen if the method can be successfully applied to rate constant calculations for realistic models of proton transfer.

The second method of solving the mixed quantum-classical Liouville equation is based on the assumption that the partially Wigner-transformed density matrix $\hat{\rho}_w$ is localized in a finite volume of classical phase space over time-scales of physical interest. The transformed density matrix is then approximated by a set of L matrices located at discrete points in classical phase space. These points, and the matrices which represent $\hat{\rho}_w$ in the region of each point, evolve in time. In the asymptotic limit of infinitely many matrices ($L \rightarrow \infty$), the evolution of the system is exact. It was demonstrated that this “localized threads” method performs very well on the proton transfer model system, and provides a controlled approach to compromising between accuracy and practicality. The applicability of the localized threads method to more interesting systems with many classical degrees of freedom is currently being investigated. One concern about applying the method to complicated systems is that the partially Wigner-transformed density matrix spreads along each degree of freedom as the system evolves. If this spread is too great, a prohibitively large number of threads must be used to represent the density matrix. However, for most weakly nonadiabatic systems, one might anticipate that most classical degrees of freedom are only weakly-coupled to the quantum subsystem so that the spread of the density matrix along only a few classical degrees of freedom is important. For this reason, we are optimistic the localized-threads algorithm will prove to be a useful prescription for performing nonadiabatic molecular dynamics calculations.

ACKNOWLEDGMENTS

The authors would like to thank Raymond Kapral and Steve Nielsen for many interesting discussions. This work was supported by a grant from the Natural Sciences and Engineering Research Council of Canada.

APPENDIX

The derivation of Eq. (30) follows in straightforward fashion by multiplying Eq. (20) on the right by the unitary matrix

$$U_{\tilde{\beta}\beta}(R) = \langle \tilde{\beta}(R) | \beta(R) \rangle, \quad (\text{A1})$$

where $\tilde{\beta}(R)$ and $\beta(R)$ are R -dependent adiabatic and force basis eigenstates, respectively, and on the left by $U^{-1}(R)$.

Letting $\tilde{\mathbf{B}}$ and \mathbf{B} denote the matrix representation of subsystem operator \hat{B}_w in the adiabatic and force basis, respectively, we observe that

$$\frac{\partial \tilde{\mathbf{B}}}{\partial R} = U^{-1}(R) \cdot \frac{\partial \mathbf{B}}{\partial R} \cdot U(R) + \left(\tilde{\mathbf{B}} \cdot U^{-1}(R) \cdot \frac{\partial U(R)}{\partial R} - U^{-1}(R) \cdot \frac{\partial U(R)}{\partial R} \cdot \tilde{\mathbf{B}} \right). \quad (\text{A2})$$

Transforming (20) and utilizing (A2), we obtain Eq. (30) with the nonadiabatic force coupling matrix given by

$$\mathbf{D} = U^{-1}(R) \cdot \mathbf{d} \cdot U(R) + U^{-1}(R) \cdot \frac{\partial U(R)}{\partial R}. \quad (\text{A3})$$

However, since

$$\left[U^{-1}(R) \cdot \frac{\partial U(R)}{\partial R} \right]_{\alpha\beta} = -[U^{-1}(R) \cdot \mathbf{d} \cdot U(R)]_{\alpha\beta} + \langle \alpha(R) | \frac{\partial}{\partial R} | \beta(R) \rangle, \quad (\text{A4})$$

the nonadiabatic force coupling matrix is simply

$$\mathbf{D}^{\alpha\beta} = \langle \alpha(R) | \frac{\partial}{\partial R} | \beta(R) \rangle. \quad (\text{A5})$$

The coupling matrix is straightforward to evaluate given that for $\alpha(R) \neq \beta(R)$,

$$\langle \alpha(R) | \frac{\partial \hat{F}_w}{\partial R} | \beta(R) \rangle = \mathbf{D}^{\alpha\beta} \cdot (\mathbf{F}_w^{\beta\beta} - \mathbf{F}_w^{\alpha\alpha}), \quad (\text{A6})$$

as can be established by evaluating the derivative of $\mathbf{F}_w^{\alpha\beta}$ with respect to R .

¹R. Kapral and G. Ciccotti, *J. Chem. Phys.* **110**, 8919 (1999).

²V. S. Filinov, S. Bonella, Y. L. Lozovik, A. V. Filinov and I. Zacharov, “Quantum molecular dynamics using Wigner representation,” in *Classical and Quantum Dynamics in Condensed Phase Simulations*, edited by B. J. Berne, G. Ciccotti, and D. Coker (World Scientific, Singapore, 1998).

³O. V. Prezhdo and P. J. Rossky, *J. Chem. Phys.* **107**, 825 (1997).

⁴J. C. Tully, *J. Chem. Phys.* **93**, 1061 (1990); J. C. Tully, *Int. J. Quantum Chem.* **25**, 299 (1991); S. Hammes-Schiffer and J. C. Tully, *J. Chem. Phys.* **101**, 4657 (1994).

⁵J. L. McWhirter, *J. Chem. Phys.* **108**, 5683 (1998).

⁶F. Webster, P. J. Rossky, and R. A. Friesner, *Comput. Phys. Commun.* **63**, 494 (1991); F. J. Webster, J. Schnitker, M. S. Friedrichs, R. A. Friesner, and P. J. Rossky, *Phys. Rev. Lett.* **66**, 3172 (1991).

⁷D. F. Coker and L. Xiao, *J. Chem. Phys.* **102**, 496 (1995).

⁸X. Sun and W. H. Miller, *J. Chem. Phys.* **106**, 916 (1997); **106**, 6346 (1997).

⁹G. Stock and M. Thoss, *Phys. Rev. Lett.* **78**, 578 (1997).

¹⁰C. C. Martens and J.-Y. Fang, *J. Chem. Phys.* **106**, 4918 (1997).

¹¹For a review of quasi-classical trajectory methods, see *Advances in Classical Trajectory Methods*, edited by W. L. Hase (Jai, London, 1992), Vol. 1.

¹²W. H. Miller, *J. Chem. Phys.* **95**, 9428 (1991); E. J. Heller, *ibid.* **94**, 2723 (1991); E. J. Heller, *ibid.* **94**, 9431 (1991); G. Stock and M. Thoss, *Phys. Rev. Lett.* **78**, 578 (1997); M. F. Herman and E. Kluk, *Chem. Phys.* **91**, 27 (1984); K. G. Kay, *J. Chem. Phys.* **100**, 4377 (1994); **100**, 4432 (1994).

¹³X. Sun, H. Wang, and W. H. Miller, *J. Chem. Phys.* **109**, 7064 (1998).

¹⁴P. Pechukas, *Phys. Rev.* **181**, 166 (1969).

- ¹⁵J. C. Tully and R. K. Preston, *J. Chem. Phys.* **55**, 562 (1971).
- ¹⁶Linear operators $i\mathcal{L}^q$, $i\mathcal{L}^{cl}$ and their sum must generate contractive semi-groups on the Banach space on which they act. In Hilbert space, this requires the spectrum of all 3 operators be purely imaginary for time reversible dynamics. For a discussion of the Trotter product formula applied to physics, see E. Nelson, *J. Math. Phys.* **5**, 332 (1964).
- ¹⁷M. N. Rosenbluth and A. W. Rosenbluth, *J. Chem. Phys.* **23**, 356 (1955).
- ¹⁸D. Frenkel, G. C. A. Mooij, and B. Smit, *J. Phys. Condens. Matter* **4**, 3053 (1991); J. I. Siepmann and D. Frenkel, *Mol. Phys.* **75**, 59 (1992).
- ¹⁹J-Y. Fang and S. Hammes-Schiffer, *J. Chem. Phys.* **107**, 8933 (1997).
- ²⁰B. Efron and R. Tibshirani, *An Introduction to the Bootstrap* (Chapman and Hall/CRC Press, London, 1993).
- ²¹For a review, see R. Kapral, S. Consta, and L. McWhirter, "Chemical rate laws and rate constants," in Ref. 2.
- ²²M. Ben-Nun and T. J. Martínez, *J. Chem. Phys.* **108**, 7244 (1998); T. J. Martínez, M. Ben-Nun, and R. D. Levine, *J. Phys. Chem.* **100**, 7884 (1996); T. J. Martínez and R. D. Levine, *J. Chem. Soc., Faraday Trans.* **93**, 940 (1997); T. J. Martínez, M. Ben-Nun, and R. D. Levine, *J. Phys. Chem.* **101**, 6389 (1997).
- ²³C. C. Wan and J. Schofield (unpublished).